Key Engineering Materials
ISSN: 1662-9795, Vol. 916, pp 222-229

Submitted: 2021-09-07
Revised: 2021-10-06
Accepted: 2021-10-28
Online: 2022-04-07

Numerical Simulations of Masonry Elements Strengthened Through Fibre-Reinforced Mortar: Detailed Level Modelling Using the OOFEM Code

Ingrid Boem[1,a*], Bořek Patzák[2,b] and Alena Kohoutková[1,c]

[1]Department of Concrete and Masonry Structures, Faculty of Civil Engineering, Czech Technical University, Thákurova 7, 166 29 Praha 6, Czech Republic

[2]Department of Mechanics, Faculty of Civil Engineering, Czech Technical University, Thákurova 7, 166 29 Praha 6, Czech Republic

[a]ingrid.boem@fsv.cvut.cz, [b]borek.patzak@fsv.cvut.cz, [c]akohout@fsv.cvut.cz

*corresponding author

Keywords: Seismic vulnerability, Masonry strengthening, Composites, FRM, CRM, Numerical modelling.

Abstract. A detailed level numerical model for Fibre Reinforced Mortar (FRM) using the free, open source code OOFEM has been recently calibrated and validated by the authors through comparison with experimental characterization tests (i.e. pull-off tests, tensile tests and shear bond tests). In this paper, the developed model is adopted to perform numerical simulations on FRM strengthened masonry elements. In particular, out-of-plane and in-plane bending tests and in-plane diagonal-compression tests are simulated by adopting the same modelling hypostasis and characteristics and the results are compared with experimental tests available in the literature. Both the masonry and the mortar are modeled through solid elements, the yarns of the fibre-based mesh with truss elements and the interactions among the components (yarns, mortar, masonry) by means of interface elements. Non-linear static analyses are performed, considering the materials and interfaces non-linearity. The simulations result capable to realistically reproduce the typical performances of masonry elements in terms of global performances and damage pattern and permit to investigate on the resisting mechanisms and on the interactions between the components.

Introduction

Fibre-Reinforced Mortar (FRM) is a modern and compatible strengthening strategy for existing masonry, which consists in plastering the walls by means of mortar layers with fibre-based elements embedded. The benefits of FRM systems have already been extensively investigated experimentally [1]-[4], but experimental tests alone do not allow to cover the whole variety of possible configurations and to reproduce accurately the actual working conditions in buildings. Numerical simulations permit to extend the experimental evidences and deeply investigate on optimized intervention and design strategies. In this context, the "conFiRMa" project [5], funded by EU's H2020 program (WF-02-2019, n.101003410), is aimed at calibrating a numerical model, validated in the free, open source finite element code OOFEM, for the assessment of the structural performances of historic masonry buildings strengthened with Fibre Reinforced Mortar (FRM). The main purpose is to develop a multiple-level approach, starting with the detailed modelling of components, followed by an optimization procedure to get a computationally efficient intermediate level model (e.g. multi-layer elements) for the calibration of the lumped plasticity model for global analysis. This paper faces with the detailed level modelling.

The investigated FRM system consists in the application of a mortar coating, about 30 mm thick, with embedded Glass Fibre-Reinforced Polymer (GFRP) meshes and L-shaped, passing-through injected GFRP connectors. This technique is also known as CRM (Composite Reinforced Mortar). The wires of the GFRP meshes are composed of Alkali-Resistant glass fibres (dry fibres cross section mm^2 in each wire). The dry fibres wires are soaked in a thermo-hardening resin made of epoxy

vinylester with benzoyl peroxide as catalyst. Then, before the resin harden, the mesh is formed by twisting the wires in one direction (warp) across the wires in the perpendicular direction (weft), which fibres remain parallels. The detailed level model for CRM was recently calibrated and validated by the authors through comparison with experimental characterization tests (i.e. pull-off tests, tensile tests and shear bond tests) [6]. It allowed investigating on the interactions among the inorganic matrix and the embedded reinforcement mesh and was proved to be capable to reproduce the behaviour of CRM samples in terms of global performances, local stresses/strains distribution and crack pattern. In this paper, the developed model is adopted to perform numerical simulations on strengthened masonry elements. In particular, out-of-plane bending tests, in plane bending tests and diagonal-compression tests are simulated and the results are compared with experimental tests available in the literature.

Modelling hypothesis

The numerical simulations are performed with the free finite element code OOFEM [7]. The 3D numerical model previously developed [6] was composed of solid elements (*LSpace,* dimensions 16.5x16.5x15 mm^3) to represent the mortar, truss elements (*truss3d,* 16.5 mm length) for the mesh wires and line-to-line (*IntElLine*) and point-to-point (*IntElPoint*) interface elements to consider, respectively, the interactions between the wires and the mortar and between orthogonal wires. Now, solid elements (*LSpace,* dimensions 16.5x16.5x15.6 mm^3) are introduced to simulate the masonry, assumed homogeneous and isotropic, and surface interfaces (*IntElSurfTr1*) to connect the mortar matrix with the masonry substrate. Nonlinear-static analyses at displacement control are performed considering the material/interface nonlinearities (Newton-Rapshon solver, with relative displacement and force convergence norms set to 10^{-3}).

The numerical model is outlined in Fig. 1 and the main material/interface properties are summarized in Table 1-2 (for unspecified parameters, the OOFEM default values are used [8]).

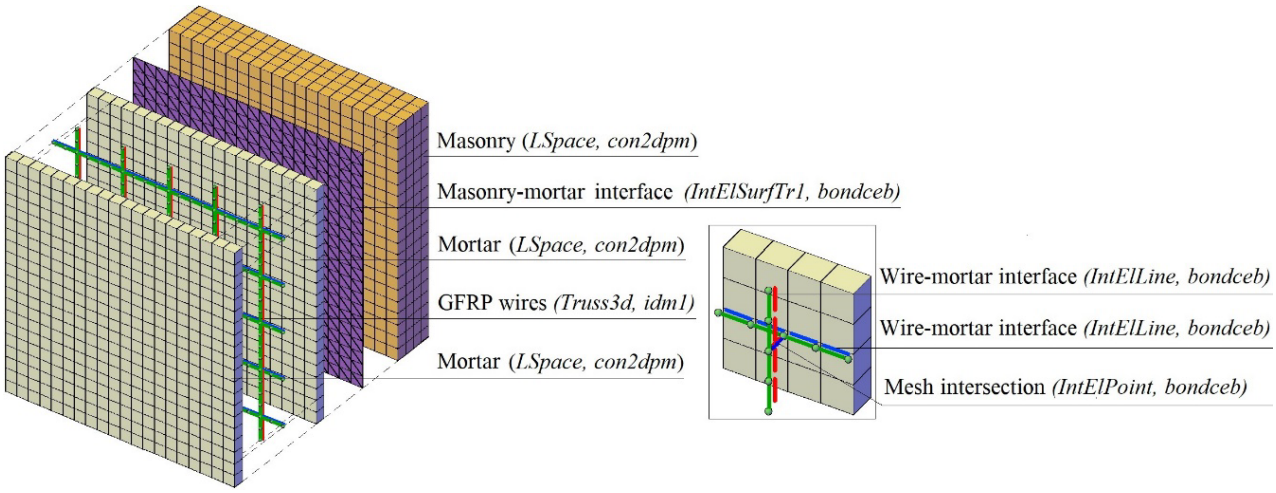

Fig. 1. Schematization of the detailed level OOFEM numerical model for the analysis of CRM strengthened masonry elements.

Table 1. Main parameters adopted for the materials in the numerical simulations.

	Mortar	Masonry
Element type	LSpace	LSpace
Material type	con2dpm	con2dpm
Young mod. E	14.4 GPa	4.27 GPa
Poisson mod. n	0.25	0.45
Comp.strength f_c	6.29 MPa	5.12 MPa
Tens.strength f_t	1.10 MPa	0.32 MPa
Softening law	linear	linear
Hardening parameters b_h , h_p	0. 002, 0.0	0.003, 0.0
Softening parameters w_f/h, a_{soft}	0.011, 1.5	0.0001, 5.0
Dilation ψ	0.85	0.58

	Twisted wire	Parallel wire
	Truss3d	Truss3d
	idm1	idm1
	62.9 GPa	69.5 GPa
	0.3	0.3
Peak strain ε_0 [%]	1.879%	2.123%
Ultimate strain ε_f [%]	1.9%	2.2%
	linear	linear
Cross section A	3.8 mm^2	3.8 mm^2

Table 2. Main parameters adopted for the interfaces in the numerical simulations.

		Wire-mortar interface		Wire intersections		Mortar-masonry
		Twisted wire	Parallel wire	Twisted wire	Parallel wire	
Element type		IntElLine	IntElLine	IntElPoint	IntElPoint	IntElSurfTr1
Material type		bondceb	bondceb	bondceb	bondceb	bondceb
Thickness t		9.57 mm	18 mm	-	-	-
Normal stiff. k_n		1000 N/mm^2	1000 N/mm^2	0 N/mm	0 N/mm	10000 N/mm^2
Tangential stiff. k_t		1000 N/mm^2	1000 N/mm^2	10000 N/mm	10000 N/mm	120 N/mm^2
Bond param.	τ_{max}	3.30 MPa	2.00 MPa	458.0 N	550.0 N	1.18 MPa
	τ_f	2.20 MPa	0.25 MPa	0.0 N	0.0 N	0.10 MPa
Slip parameters	s_1	0.1 mm	0.1 mm	0.5 mm	0.5 mm	0.02 mm
	s_2	0.1 mm	0.1 mm	1.5 mm	0.5 mm	0.11 mm
	s_3	1.2 mm	1.2 mm	10.0 mm	0.6 mm	0.80 mm

For the mortar, the GFRP wires and the mesh intersections, the outcomes of laboratory characterization tests were considered and the wire-mortar interface were calibrated from pull-out tests [6]. A Concrete-Damage Plasticity model [9] is calibrated for the masonry, so to account for both crushing and cracking, with characteristics set in accordance to the experimental results of compression and diagonal compression tests on plain masonry elements, respectively. The mortar-masonry interaction accounts for the possible debonding, emerged from some shear-bond experimental tests [10].

Experimental evidences

Several experimental tests on CRM strengthened masonry elements were performed in the recent past. In particular, the results herein summarized refer to out of-plane bending tests, in-plane bending tests and diagonal compression tests performed of single wythe, solid brick masonry, 250 mm thick (nominal compressive resistance of about 44 MPa for the bricks and 2.9 MPa for the lime mortar), strengthened by means of a 66x66 mm^2 GFRP mesh embedded in a layer of mixed lime and cement mortar (mean compressive and tensile strengths about 6.3 and 1.1 MPa, respectively). The capacity curves are reported in the following section, in comparison with the numerical results.

Out of-plane bending tests. Four-point bending tests (label "OB") concerned masonry samples 1000x3000x250 mm^3, vertically arranged and strengthened with CRM at both faces (GFRP twisted fibres wires disposed in the vertical direction) [11]. Unreinforced masonry was also tested, as reference. The samples were provided with a vertical support at the base and horizontal constraints at the top and at the bottom, on the front side. Two hydraulic jacks, connected in parallel, provided the horizontal loading at the thirds of the height, on the back side. Loading-unloading cycles were performed until the attainment of the first cracking; then the tests were prosecuted with monotonic loading.

The unreinforced sample performed almost elastically till the first cracking, at about the mid span, at the front side (Fig. 2a); a sudden resistance reduction occurred and a residual load, related to the rocking kinematic mechanism, was experienced. In the CRM strengthened sample, the first cracking appeared horizontally in the mortar coating, in the mid-third of the height, on the front side; then, other parallel cracks progressively formed in this area (Fig. 2b), accompanied by some drop of resistance and a subsequent increase. A global hardening was recognized in the load-deflection behaviour, till the attainment of the collapse, due to the tensile rupture of the vertical GFRP wires in correspondance of a crack.

Fig. 2. Out-of-plane bending tests: damage pattern of (a) plain and (b) CRM strengthened masonry.

In plane bending tests. Three point bending tests (label "IB") concerned solid brick masonry wallets (780x380x250 mm^3), pre-loaded with axial stress level σ = 0.15 MPa and then subjected to loading-unloading cycles (span 680 mm). The GFRP mesh had the twisted fibres wires disposed along the loading direction; an unreinforced sample was also tested, as reference.

The behaviour of the unreinforced masonry sample (Fig. 3a) was governed by the rocking kinematic mechanism and the load-deflection curves had an elastic-plastic trend (the tensile strength of the masonry resulted negligible). The load-deflection curve of the CRM strengthened sample had an initial elastic trend, until remained un-cracked; then a global hardening was detected, since the first cracking appeared vertically in the mortar coating, at about the mid span and other cracks progressively formed in the vicinity, with a vertical trend in the lower part and an inclined trend in the upper portion (Fig. 3b). The failure was due to the tensile failure of the GFRP wires, in the lower part, which opposed to the free rocking until breakage, at about 3.65 mm deflection.

Fig. 3. In-plane bending tests: damage pattern of (a) plain and (b) CRM strengthened masonry.

Diagonal-compression tests. The diagonal compression tests (label "DC") concerned solid brick masonry panels, 1160x1160x250 mm^3 [12]. The samples were arranged on a vertical support and metallic stiff devices were installed at two opposite corners, to apply the diagonal compression. Loading-unloading cycles were performed, monitoring the compressive and tensile diagonal strains.

Unreinforced samples (Fig. 4a) developed an approximately linear trend almost up to the peak load; then, a sudden drop in resistance occurred after the appearance of a diagonal cracking. In general, the cracks had a stair-stepped pattern; the residual load was related to friction between elements across the cracks and to the compressive strength of the masonry struts. CRM strengthened samples (Fig. 4b) behaved elastically since a diagonal crack formed in the mortar coating, just before reaching the peak load. Then, the cracking zone progressively spread, with the formation of other cracks, and cracking involved also the masonry. The decrease of resistance resulted quite gradual; the progressive collapse of several GFRP wires in the widely damaged area occurred from values of diagonal tensile deformation ε_t of about 0.5-0.6%; a diffuse damage of the mortar among cracks was also observed (also with local detachments of mortar portions covering the GFRP mesh).

Fig. 4. Diagonal compression tests: damage pattern of (a) plain and (b) CRM strengthened masonry.

Numerical Results and Comparisons

Out of-plane bending tests. For the detailed level numerical model, since not relevant bi-dimensional bending effects were monitored during the experimental tests, only one vertical through-the-thickness strip (66 mm width) is considered. The horizontal displacements are constrained at the top and at the bottom supports (front face). At the base, the vertical displacement is avoided at the mid thickness and a spring element are introduced to account for steel-to-steel friction (element type: *IntElPoint*, cross section type: *InterfaceCS*, material type: *SimpleInterMat*, coefficient of static friction 0.8). The self-weight, in the vertical direction, is at first applied and maintained constant; then, the horizontal load is applied through two forces at the thirds of the height (back side). Displacement control is performed by prescribing the horizontal displacement increments at the midspan. The numerical results are reported in Fig. 5a in terms of load - deflection curves, in comparison with the experimental results. Generally, the experimental behaviour is catch with good accuracy by the model. In the unstrengthen samples, a single crack occurs at about 2/3 of the height (Fig. 5b), inducing a sudden drop of resistance. In the CRM strengthened one (Fig. 5c), as the deflection increases, multiple cracks form sequentially in the central third of the height and the GFRP vertical wires oppose to the free cracks opening, till failure.

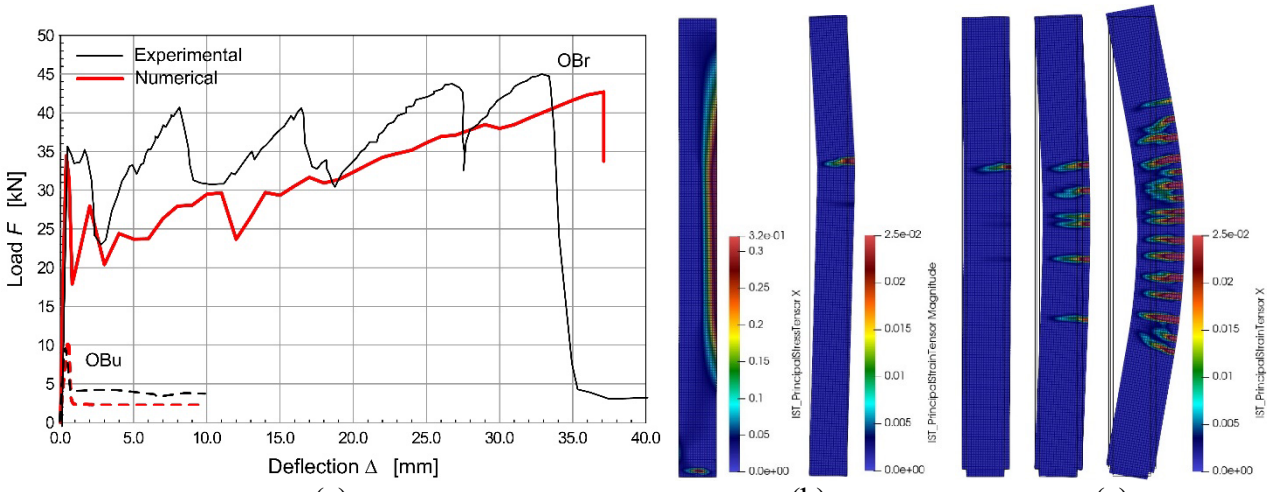

(a) (b) (c)

Fig. 5. Out-of-plane bending: (a) load-deflection curves, (b) principal tensile stresses at first cracking and principal tensile strains at Δ = 2.0 mm for the unreinforced sample, (c) evolution of the principal tensile strains at Δ= 1-10-38 mm.

In plane bending tests. Due to the sample symmetry, only one fourth of the specimen is considered for the detailed level numerical model. The vertical displacements are constrained at the mid width of the steel support plates. Horizontal forces are at first applied at the free end and maintained constant, to represent pre-compression loading; then, the vertical displacement is applied in correspondance of the top steel plate, at the mid span.

The load deflection curves, plotted in Fig. 6a, follow adequately the trend of the experimental samples. The simulations confirm that the first crack is due to bending and occurs at the intrados, in correspondance of the mid span. Then, in the plain samples (Fig. 6b), the kinematic mechanism activates due to the presence of the compressive load. In strengthened samples (Fig. 6c), the presence of the GFRP wires crossing the crack opposes to its opening and allows the load increase, even though a marked stiffness reduction is detected. Other cracks originate from the intrados; the slope tends to vary in the upper portion of the sample, due to shear stresses and a further reduction in stiffness is observed. The maximum load is attained when the ultimate deformation is reached in the horizontal wire at the intrados, at the mid span. The lower ultimate deflection in the experimental tests is realistically related to a reduced resistance of the GFRP wire in respect to the mean value.

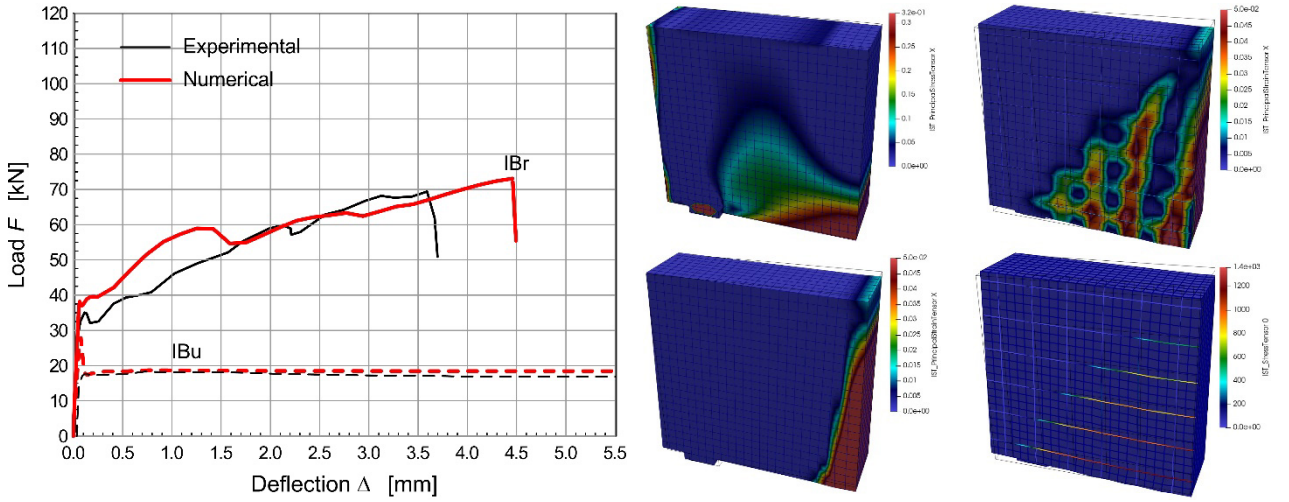

(a) (b) (c)

Fig. 6. In plane bending: (a) load-deflection curves, (b) principal tensile stresses at first cracking and principal tensile strains at $\Delta = 2.0$ mm for the unreinforced sample, (c) principal tensile strains and tensile stresses in the GFRP mesh for the CRM strengthened sample just before failure.

Diagonal-compression tests. One eighth of the specimen is considered for the detailed level numerical model, to reduce the computational effort (the asymmetric effect of the self-weight is assumed negligible with respect to the considered load levels). The diagonal displacement is applied in correspondance of the corner steel bracket. The numerical results are plotted in Fig. 7a in load – diagonal strains curves.

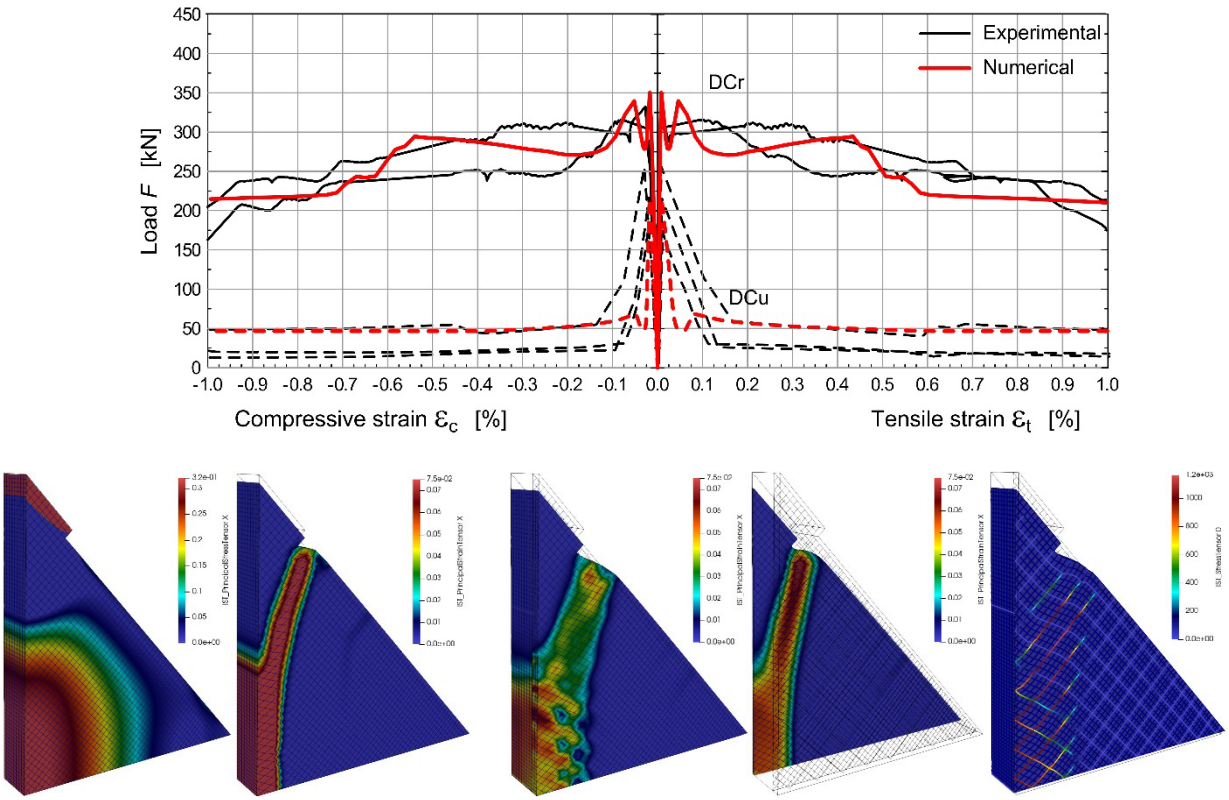

Fig. 7. Diagonal compression: (a) load-diagonal strains curves, (b) principal tensile stresses at first cracking and principal tensile strains at ε_t = 0.45% in the unreinforced sample, (c) principal tensile strains in the mortar coating and in the masonry and tensile stresses in the GFRP mesh, just before failure in the CRM strengthened sample (ε_t = 0.45%).

The unreinforced sample (Fig. 7b) experiences an abrupt drop down of resistance just after the attainment of the first cracking in the panel centre; the damage propagates rapidly along the compressed diagonal and a pushing masonry wedge originates around the corner device. In the CRM strengthened sample (Fig. 7c) a first peak load is detected as the tensile resistance in the mortar coating and in the masonry are reached, almost simultaneously, in the centre of the panel. At the increasing of the applied displacement, the damage gradually spreads; actually, in respect to the masonry, the damaged area in the mortar coating is wider and the tensile strains are lower. The failure of the GFRP wires starts at about ε_t = 0.45% and determines a drop of resistance. The load decrease is more gradual in the experimental curves, but this is reasonably due to the scatter in the GFRP wire resistance, in respect to the mean value assumed in the simulations. Such a difference emerges more clearly in this test, since wide portions of the GFRP mesh are affected by high tensile stresses.

Discussion and Conclusions

In this paper, the detailed level numerical model previously crated and validated by the authors using the OOFEM code has been applied to simulate the behaviour of CRM strengthened masonry elements subjected to out-of-plane and in plane actions. The 3D model accounts for the non-linearity of the materials and the interfaces, whose properties were calibrated only once on the basis of experimental characterization tests and are used in all simulations herein presented. The main experimental outcomes of previous tests on CRM strengthen masonry elements (bending and diagonal compression tests) are resumed and used for comparison with the numerical results.

Generally, the model is capable the reproduce all the typical failure modes of CRM strengthened masonry elements (out-of-plane and in-plane bending and diagonal cracking) and the results of the non-linear analyses are proved to be reliable also at advanced damage level. The main discrepancy in the comparisons with the experimental outcomes may be attributable to uncertainties in the material

properties, mainly in the tensile strengths of the masonry, the mortar matrix and of the GFRP wires, which can actually be affected by significant variations in respect to the nominal values assumed in the numerical models. Moreover, it has to be observed that the simulations, with monotonic loading, neglect possible cumulative damage due to the loading-unloading procedure adopted experimentally. It addition, it should be considered that the experimental setups did not allow precise "displacement control" tests, as the numeric simulations permit.

A sensitivity analysis is in progress, to assess the main material parameters influencing the results, varying the reinforcement ratio, the matrix characteristics, the interfaces performances and also considering masonry of different type and thickness. The results will allow a robust definition of the FRM behaviour for the intermediate level modelling, based e.g. on multilayer elements, which will be adopted for the simulation of entire strengthened walls and structures.

Acknowledgment(s)

The project “conFiRMa” has received funding from the European Union’s Horizon 2020 research and innovation program (WF-02-2019, n.101003410).

References

[1] C. Papanicolaou, T. Triantafillou, M. Lekka, Externally bonded grids as strengthening and seismic retrofitting materials of masonry panels, Constr. Build. Mater. 25 (2011) 504–514.

[2] A. D’Ambrisi, M. Mezzi, A. Caporale, Experimental investigation on polymeric net-RCM reinforced masonry panels, Compos. Struct. 105 (2013) 207–215.

[3] N. Ismail, J.M. Ingham, In-plane and out-of-plane testing of unreinforced masonry walls strengthened using polymer textile reinforced mortar, Eng. Struct. 118 (2016) 167–177.

[4] L.A.S. Kouris, T.C. Triantafillou, State-of-the-art on strengthening of masonry structures with textile reinforced mortar (TRM), Constr. Build. Mater. 188 (2018) 1221–1233.

[5] https://sites.google.com/view/confirmaproject

[6] I. Boem, B. Patzák, A. Kohoutková, Calibration of a numerical model for Fibre-Reinforced Mortar analysis with OOFEM code, Int. Conf. of Steel and Composite for Engineering Structures - ICSCES, 12 - 13 July 2021, Ancona, Italy.

[7] B. Patzák, OOFEM - an Object-oriented Simulation Tool for Advanced Modeling of Materials and Structures, Acta Polytech. 52, 6 (2012) 59–66.

[8] http://www.oofem.org

[9] P. Grassl, M. Jirásek, Damage-plastic model for concrete failure, Int. J. Solids Struct. 43, 22–23 (2006) 7166-7196.

[10] N. Gattesco, and I. Boem, Characterization tests of GFRM coating as a strengthening technique for masonry buildings, Compos. Struct. 165 (2017) 209–222.

[11] N. Gattesco, I. Boem, Out-of-plane behavior of reinforced masonry walls: Experimental and numerical study, Compos. B Eng. 128 (2017) 39–52.

[12] N. Gattesco, I. Boem, Experimental and analytical study to evaluate the effectiveness of an in-plane reinforcement for masonry walls using GFRP meshes, Constr. Build. Mater. 88 (2015) 94–104.